AD-A190 716 THE INTERACTION OF SMALL PARTICLES WITH LASER BEAMS(U) 1/1
FLORIDA UNIV GAINESVILLE SPACE ASTRONOMY LAB
N V MISCONI ET AL 17 DEC 87 AFOSR-TR-87-2043
UNCLASSIFIED F49620-85-C-0117 F/G 20/6 NL

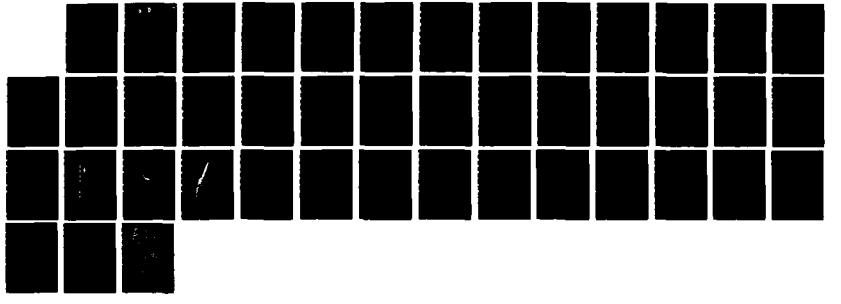

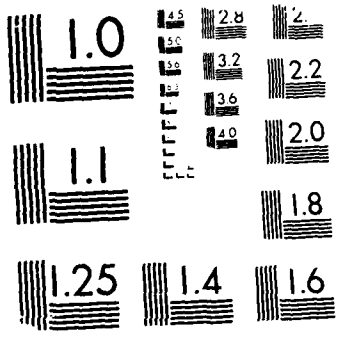

SECURITY CLASSIFICATION OF THIS PAGE

REPORT DOCUMENTATION PAGE

AD-A190 716

1b RESTRICTIVE MARKINGS	DTIC FILE COPY
2b DECLASSIFICATION / DOWNGRADING SCHEDULE	3 DISTRIBUTION / AVAILABILITY OF REPORT: Approved for public release; distribution unlimited.
4 PERFORMING ORGANIZATION REPORT NUMBER(S): UF-D	5 MONITORING ORGANIZATION REPORT NUMBER(S): AFOSR-TR. 87-2043
6a NAME OF PERFORMING ORGANIZATION: University of Florida	6b OFFICE SYMBOL (If applicable):
7a NAME OF MONITORING ORGANIZATION: AFOSR-~~86-0083~~	
6c ADDRESS (City, State, and ZIP Code): Space Astronomy Laboratory, 1810 NW 6th Street, Gainesville, FL 32609	7b ADDRESS (City, State, and ZIP Code): Bldg 410, Bolling AFB, D.C. 20332
8a NAME OF FUNDING / SPONSORING ORGANIZATION: AFOSR-~~86-0083~~	8b OFFICE SYMBOL (If applicable): NE
9 PROCUREMENT INSTRUMENT IDENTIFICATION NUMBER: F49620 85-C 0117	
8c ADDRESS (City, State, and ZIP Code): Bldg 410, Bolling AFB, D.C. 20332	10 SOURCE OF FUNDING NUMBERS: PROGRAM ELEMENT NO 61102F; PROJECT NO 2306; TASK NO A2; WORK UNIT ACCESSION NO

11. TITLE (Include Security Classification)

The Interaction of Small Particles with Laser Beams

12 PERSONAL AUTHOR(S)
Dr. N. Y. Misconi, Dr. K. F. Ratcliff, and Dr. E. T. Rusk

13a TYPE OF REPORT	13b TIME COVERED	14 DATE OF REPORT (Year, Month, Day)	15 PAGE COUNT
Annual	FROM Oct. 86 TO Oct. 87		

16 SUPPLEMENTARY NOTATION

17 COSATI CODES			18 SUBJECT TERMS (Continue on reverse if necessary and identify by block number)
FIELD	GROUP	SUB-GROUP	

19 ABSTRACT (Continue on reverse if necessary and identify by block number)

This report summarizes our research under Award/Contract F49620-85-C-0117 which deals with light scattering measurements of levitated spherical and irregular particles in an Argon laser beam (effective wavelength, 514.5 nm) of highly transparent silica. The particles range in size from 25-55 microns in diameter. Comparisons between the measurements (for scattering angles θ = 27 - 162°) and computed theoretical Mie scattering curves are made. Preliminary results on rotating irregular particles are included.

20 DISTRIBUTION / AVAILABILITY OF ABSTRACT	21 ABSTRACT SECURITY CLASSIFICATION
☐ UNCLASSIFIED/UNLIMITED ☐ SAME AS RPT ☐ DTIC USERS	
22a NAME OF RESPONSIBLE INDIVIDUAL: ~~Dr. N. Y. Misconi~~ Dr. K. Ratcliff	22b TELEPHONE (Include Area Code): (202) 767-4933
22c OFFICE SYMBOL: NE	

DD FORM 1473, 84 MAR — 83 APR edition may be used until exhausted. All other editions are obsolete.

SECURITY CLASSIFICATION OF THIS PAGE

ANNUAL REPORT

AFOSR CONTRACT - F49620-85-C-0117

THE INTERACTION OF SMALL PARTICLES WITH LASER BEAMS

Period of performance: 10 Oct. 1986 - 9 Oct. 1987

Principal Investigator:
Dr. N. Y. Misconi
Space Astronomy Laboratory
University of Florida
1810 NW 6th Street
Gainesville, Florida 32609
(904) 392-5450

Co-Investigators:
Dr. K. F. Ratcliff
Department of Physics
State University of New York
at Albany
1400 Washington Avenue
Albany, New York 12222

Dr. J. P. Oliver
Department of Astronomy
University of Florida
Gainesville, Florida 32611

Dr. E. T. Rusk
Space Astronomy Laboratory
University of Florida
1810 N. W. 6th Street
Gainesville, Florida 32609

December 17, 1987

AFOSR-TR- 87-2043

Annual Report

AFOSR Contract - F49620-85-C-0117

PREFACE

The results presented here are preliminary. A more complete analysis of the scattering measurements will be included in the final report on this contract.

PART ONE: INTRODUCTION

This annual report summarizes our research under Phase Two of Award/Contract F49620-85-C-0117 in which we concentrate upon the scattering of radiation by single particles or by small clusters of particles resulting from the attachment of one or more much smaller particles onto the surface of a larger particle. The scattering experiments utilize the 514.5 nm green line of a 20 watt TEM mode CW argon laser. The particles are all glasses or fused silicas which are highly transparent (absorption coefficient in range from 5×10^{-2} to 5×10^{-4} cm^{-1}) over the extended visible range of wavelengths to which the atmosphere is also transparent (220 - 2200 nm). The particles range in size from 15 - 100 microns. The particles are thus large compared to the wavelength of the radiation and may be said to be in the size range of geometrical optics.

In Part Two of this annual report we describe the experimental procedure used in making these scattering measurements. Part Three contains a summary of our results and compares the angular distribution of the intensity of the scattered light with that predicted by Mie calculations of scattering from spheres of the same size. A final summary together with suggestions of future research directions is contained in Part Four of this report.

PART TWO: OVERVIEW OF THE EXPERIMENT

To the best of our knowledge, the measurements reported below represent the first time that the angular distribution of radiation scattered from a particle has been measured under conditions in which the particle was supported by the pressure arising from the same radiation that was scattered. We describe below this novel approach which allows the investigation of scattering by genuinely irregular particles.

A vertically directed laser beam was used to create an optical trap, i.e. an equilibrium position for a transparent particle in which it was stably levitated by the radiation pressure from the laser beam. In the size range of geometrical optics, transparent particles that roughly resemble spheres will, to a first approximation, behave like converging lenses. This observation immediately identifies

the direction of the reaction force exerted on the particle by the radiation whose momentum is altered by passage through the particle (fig. 1). In particular there will be a force component on the particle transverse to the beam which will drive the particle toward the axis of a gaussian mode laser beam. The longitudinal force component will be in the downstream direction of the laser beam. The equilibrium position in this direction is established by bringing the vertically directed laser beam to a focus below the particle. The vertical force on the particle thus decreases with distance above the focus and the equilibrium position is established at that point along the beam where the vertical component of the radiation force is balanced by gravity.

The examples of results which are quoted in Part Three below employ low-absorbing silica particles ranging in size from 25 to 55 microns in diameter. The laser power employed in the levitation of these particles ranged from 1 to 5 W in the 514.5 nm green line. A long focal length lens (5 cm) guarantees strong transverse confinement of the particle. At the position of the particle in levitation, the 1/e width of the Gaussian profile is typically 5-6 times the particle diameter. The radiation field seen by the particle at its levitated position is thus reasonably constant across the particle. The radiation intensity at the position of the levitated particle is typically on the order of 10 kW/cm2.

In Figure 2 we show our design of the mechanical components which are the key to the success of the scattering experiment. These components are housed within a cylindrical scattering chamber 14 cm in diameter and 13 cm high. The scattering chamber serves to isolate the levitated particle from air currents, which frequently exceed the strength of the radiation pressure on the particle. Prior to levitation, the particle sits on a launching plate - a thin glass cover plate mounted on top of a piezoelectric cylinder. The incident laser beam passes through the launching plate. Vibration of the launching plate breaks the Van der Waals force binding the particle to the plate. The focus of the laser beam is placed just below the particle so that the particle will move to the position of stable levitation after release from the plate. Upon achieving levitation, the launching plate is lowered along the beam axis to the bottom of the scattering chamber. This enables us to extend our scattering measurements well into the backward hemisphere.

Intensity as a function of scattering angle is measured by a goniometer which contains in one arm a photodiode whose field of view is confined to a width of 2 degrees. On the opposite arm and facing the photodiode is a light baffle which, through a combination of multiple scattering and black anodized surfaces, guarantees that stray light entering the photodiode is at least one order of magnitude below the minimum intensity of the particle. Limits on the

excursion of the goniometer, and therefore on the range of observed scattering angles, are established by movement of either the photodiode shield or the baffle into the launching plate in its lowered position or into the laser beam itself. With the present design, we cover a range of scattering angles from 27 to 162 degrees (from the forward direction).

With the particle in its levitated position, we monitor the particle in a variety of ways.

1. We obtain the near field image of the particle in the forward direction and project that image onto a screen. If our particle were a perfect sphere that image would look like a doughnut with a bright center of undeviated rays surrounded by a dark ring in which light has been removed from the forward direction. The presence of surface irregularities in either of the polar regions will alter the bright center in our image and, as such, provides us with a measure of the irregularity of the particle. Large (> 1 um) surface irregularities will be visible on this image. The near field image is also used to measure the size of the levitated particle.

2. A transparent section in the top of the scattering chamber allows us to view the far field scattering pattern over a range of a few degrees centered about the 15 degree scattering angle. A perfect homogeneous

sphere would produce an image consisting of concentric rings of local maxima and minima in the intensity pattern. During levitation of particles with surface irregularities we have observed shadows, i.e. regions of reduced intensity, to interrupt this pattern. If the particle rotates about the beam axis (a frequent occurrance for irregular particles due to radiometric forces on their surface) then the rotation of this far field pattern can be used to measure the rotation frequency of the particle. That rotation is also being monitored by the goniometer. However if that rotation is not periodic then the naked eye view of this far field view on the ceiling of the laboratory will give a much more rapid interpretation of the global behavior of the particle.

3. Through a glass window in the side of the scattering chamber, we project a near field image of the particle as seen at a 90 degree scattering angle onto the same screen containing the near field image at 0 degrees. If the particle were a perfect sphere, then the near field image at 90 degrees will consist of a pair of bright spots - one being due to reflection from the external surface and the other being due to a pair of refractions. These bright spots emerge from the surface separated by about 68 % of the diameter of the sphere. Surface irregularities will complicate this otherwise simple 2 spot pattern. Departures from this

pattern are easily followed as the particle rotates. This 90 degree image is used to monitor the vertical position of the particle in the laser beam. As the particle rotates it will expose its surface in a variety of orientations relative to the beam axis. The resulting changes in the scattering will cause changes in the radiation force exerted on the particle and thus changes in the position of equilibrium along the beam axis. Normally the vertical excursion of the particle does not exceed 3 particle diameters. Such small translations (corresponding to an angular motion of less than 0.2 degrees) along the beam axis keeps the particle well within the 2 degree field of view of the goniometer. On ocassion the vertical excursion of the particle can exceed 10 particle diameters.

4. Both the 0 degree and 90 degree near field images are projected on a common screen and that screen is imaged by a television camera with the images stored on videotape. When the particle surface is complex, we will see a combination of rotation and translation along the beam axis. This complex motion is resolved by superimposing a timing signal on the videotape so that the motion can be advanced frame by frame at intervals of 3/100 seconds.

The scattering experiments reported below were done at ambient atmospheric pressure in the scattering chamber. We

are able to exploit the ambient pressure in two important ways. Surface irregularities on the particle mean that the radiation intensity in the vicinity of the particle surface is not cylindrically symmetric about the beam axis. This in turn causes asymmetry in the temperature and thus in the radiometric forces exerted on the particle. The typical response of the particle is to rotate about an axis that makes a small angle with respect to the beam axis. If this rotation changes the particle orientation in the incident beam then the equilibrium position of the particle changes along the beam axis. This means that the rotation may be accompanied by a periodic translation along the beam axis by an amount typically 2 or 3 particle diameters. Thus the ambient pressure is being used to rotate the particle. This causes the signal picked up by the photodiode to be averaged over all the surfaces brought within its field of view.

The second use made of the ambient pressure is to damp the motion of the particle. This ensures that the particle moves quickly to its equilibrium behavior after release from the launching plate. It also places a limit on the frequency of rotation of the particle - typically 1 or 2 Hz and only rarely exceeding 8 Hz in our observations. Perhaps the most important argument for performing the scattering measurements at ambient pressure is that the damped particle is more stable than it would be at lower pressure, allowing us to use particles or clusters of particles which depart more strongly from spherical shapes.

PART THREE: DISCUSSION OF RESULTS

The scattering of electromagnetic radiation by perfectly spherical particles has long been accurately calculated by the Mie theory. The prediction of the Mie theory depends on the incident radiation's state of polarization, the index of refraction, and the ratio of sphere circumference to wavelength which defines the "x-parameter" or "size parameter" of Mie theory. The glasses we have used fall into two groups, having indexes of 1.46 and 1.52. Our range of particle sizes from 15 to 100 microns covers size parameters from $x = 92$ to $x = 611$ (wavelength = 514.5 nm) a range not usually subject to experimental investigation. For direct comparison to Mie theory we are effectively limited to a particle size of no more than 70 microns ($x = 427$) since our 20 W argon laser is limited to 7.5 W in the green line. Only multiline operation of the laser will suffice for levitation of the larger particles.

With such a large size parameter, the Mie scattering pattern of a transparent particle (negligible imaginary part of index of refraction) oscillates rapidly in amplitude with changing scattering angle, and with small angular separation of the maxima. This is shown in Figure 4 for a sphere of diameter 39.6 microns (the accuracy of this size, provided by the manufacturer, is questionable; the

corresponding size parameter x = 242) and refractive index = 1.519. Also shown in Figure 4 (the dark line running through the oscillations) is an averaged Mie pattern in which the smoothing is achieved by averaging over a 2 degree interval. This interval represents the field of view of our photodiode mounted in our goniometer. The smoothing that results is considerable since 2 degrees typically includes 3 complete oscillations of the intensity curve. In all of the comparisons below of experiment with theory (of a perfect sphere of equal size) we shall employ the 2 degree angle averaged Mie pattern as the theoretical curve.

EXAMPLES OF PARTICLES THAT ARE SPHERICAL

We begin with the case of spherical particles. Comparison of experiment and Mie theory for spheres serves as a quality control on our experiment. In Figure 5 we show the scattering by a 33 micron sphere of fused silica (index of refraction = 1.459). The incident beam is linearly polarized (> 99%) in a direction 37 degrees from the normal to the scattering plane. The agreement between experiment and Mie scattering is quite good. The number, relative heights, and angular location of the maxima between 80 and 110 degrees are well reproduced in our measurements. The onset of the sharp rise beyond 150 degrees is within 3 degrees of the theoretical prediction. The intensity below

45 degrees is systematically smaller than that predicted by theory. The reason for this is still being determined.

The scattering of light is strongly dependent on the state of polarization. In Figure 6a we show our data for the 33 micron sphere compared to the case of zero polarization angle (i.e. the electric field vector lies normal to the scattering plane). In Figure 6b we extend this comparison to the case of 90 degrees polarization angle (i.e. the electric field vector lies in the scattering plane). The structure near 90 degrees and sharp rise at 150 degrees are seen in Mie scattering for 0 degrees polarization but are absent for 90 degrees polarization. The decrease in angle-averaged intensity with scattering angle in the forward hemisphere falls more slowly in the case of the 90 degrees polarization. In the case of our data for 37 degrees polarization, the ratio of peak to valley in the structure in the neighborhood of 90 degrees scattering angle is much higher for 0 degrees polarization Mie scattering than for 37 degrees polarization Mie scattering. This point is immediately made by comparing the fit of our empirical data to theory in Figures 6a and 6b. This seems to be an aspect of our scattering experiments which is most sensitive to polarization angle.

We turn next to the sensitivity of our measurements to the index of refraction of the transparent particles we employ. We worked with a source of accurately

sized transparent glass spheres, 39.6 microns in diameter. The supplier of these spheres was however not able to provide any information on the index of refraction of the spheres. Mie scattering from spheres depends only upon the polarization angle, the size parameter, and the index of refraction. Since the polarization angle (37 degrees) and the size parameter ($x = 242$) were well known, the challenge to us was to see if the scattering data could be used to determine the index of refraction.

In Figures 7a through 7c we superimpose our empirical data on Mie scattering curves over a narrow range of the index of refraction. We see immediately that the location and the relative magnitude of the maxima and minima in the neighborhood of 90 degrees scattering angle is very sensitive to small changes in the index of refraction. This is to be expected for particles of such a large size parameter since a small change in the index of refraction can cause a large change in the optical path (more accurately in the phase) across the particle. In the present case, the scattering data identifies our index of refraction to be in the neighborhood of 1.52.

EXAMPLES OF IRREGULAR PARTICLES THAT ACT LIKE SPHERES

In this section we give three examples of irregular particles that act like spheres in that they are stable in their levitated position. These particles do not rotate. The only observed motion of the particle is an oscillation

about the beam axis of less than 10 degrees. This is accompanied by vertical motion of a small fraction of one particle diameter. Irregularities on the surface of these particles is not visible in the near field 0 degree image. The existence of irregularities is seen in the laboratory by observing departures from the 2-spot pattern in the 90 degree near field image and/or dark patterns which have irregular longitudinal components in their shape as seen in the far field image at about 15 degrees scattering angle.

The first of these examples is shown in Figure 8. This is the case of a 25 micron particle which was extremely stable. The similarity to a sphere is seen in the rate of decreasing intensity with increasing angle up to 80 degrees and the amplitude of the relatively flat intensity between 110 and 150 degrees. The rise beyond 150 degrees also agrees with the underlying spherical shape. In the structure between 80 and 110 degrees, the departure from the theoretical curve is most likely due to the uncertainty in the measurement of particle size. Since we are limited to optical methods, there is a probable error of +/- .5um in making this measurement (the wavelength of the light). Because of this, the observed structure in the scattering curve near 90 degrees is unlikely to match the theory. The sensitivity to size is such that a 0.1 um difference in particle diameter will result in variations comparable to those displayed in figures 7a-7c for small changes in the refractive index.

A significant departure from sphericity is seen in Figure 9 in which we have a 51 micron particle. The flat region and eventual rise in the backward hemisphere as well as the average slope of the intensity with angle below 60 degrees reflect the underlying spherical nature of this particle. We see intensity variations in the 30 to 70 degree range that are not seen in the pure sphere. But the greatest departure from sphericity is seem in the ratio of intensity in the forward hemisphere to that in the backward hemisphere. The ratio of the intensity from 30 to 60 degrees to that from 120 to 150 degrees for this particle is 1/5 of the ratio for a sphere of the same size.

The last of these examples is that of a 35 micron particle seen in Figure 10. This again was an especially stable particle in levitation but its angular distribution differs from that of the equivalent sphere in almost all respects. The ratio of intensity from 30 to 60 degrees to that from 120 to 150 degrees is again low but the effect is less than half that seen in the preceding example. The angular distribution of this particle is oscillatory below 70 degrees which is not seen for the sphere. The rise to the backward peak occurs gradually for this particle unlike that for the sphere.

IRREGULAR PARTICLES THAT STRONGLY DEPART FROM SPHERICAL BEHAVIOR IN LEVITATION

We turn next to three examples of particles which have surface irregularities which result, during levitation, in both rotation about the beam axis with periodic translation along the beam axis. In any given sample of particles, the majority of those which are regular enough to be confined in levitation by radiation pressure will be found to behave in the manner that we are about to describe.

The scattering chamber we use has a transparent plexiglass door that opens to give us access to the launching plate. That door is covered in a plastic whose color is complementary to the green line of the argon laser. This arrangement gives us a crude far field glimpse of the particle's scattering pattern as seen by the goniometer in the range from 60 to 120 degrees.

The strong departure from sphericity of these particles is immediately evident from the pattern of "shadows" seen on the door of the scattering chamber. Those shadows are elongated in a direction that would correspond to lines of longitude on the equivalent sphere. Thus rotation of the particle carries these shadows across our photodiode mounted in the goniometer. Output from that photodiode is imaged as an electronic strip chart on the screen of our VME/10 computer. The output of the photodiode is sampled 100 times each second.

The periodic passage of these patterns of brightness and shadows through the photodiode is recorded as a periodic intensity pattern seen at a fixed scattering angle. On our plots below, the empirical data represents intensities averaged over the various orientations seen at fixed scattering angles. We only present results from particles which rotated with a constant angular velocity and for which the time average was therefore a uniform average over particle orientation about the beam axis. The number of maxima in the intensity, that are recorded at a fixed scattering angle, typically run from 5 to 30 per complete rotation. In addition to recording the average intensity, we also record the extreme maximum and extreme minimum intensity seen at fixed scattering angle over a few rotational periods. These irregular particles have fluctuations in intensity (at fixed scattering angle) such that the ratio of extreme maximum/extreme minimum typically ranges from 3 to 12 or more. (By contrast, the more "spherically behaving" particles, discussed in earlier sections of this report, yield values of extreme maximum/extreme minimum that typically range from 1.05 to 1.50.)

Our experience is that 60% of the particles we levitate will rotate about the beam axis, periodically translate along the beam axis, and display an intensity variation at fixed scattering angle which is typified by the discussion above. It is then of interest to ask whether the "average"

behavior of such rotating irregular particles will resemble that of a sphere of equivalent size.

We look first at Figure 11 which shows a 45 micron sphere which rotated at 1 Hz and translated by 2 particle diameters (not sufficient to have much influence on the scattering angle). While the empirical data may be argued to be somewhat smoother than that of a sphere, there is no question that the rotationally averaged behavior of this particle resembles that of the equivalent sphere rather closely.

A very different conclusion is reached when we look at Figure 12 which gives the results for a 55 micron particle. This particle oscillated very rapidly along the beam axis with an amplitude of 3 particle diameters. This particle exhibited a second mode of behavior in which the oscillation amplitude decreased but was then accompanied by a 1 Hz rotation. Beginning with the strong peak recorded near 90 degrees (which looked like a rotating lighthouse beacon in the near field 90 degree image) and extending across the backward hemisphere, the rotationally averaged behavior is somewhat "spherical". But the forward hemisphere is characterized by an enormous peak at 30 degrees followed by a flat intensity profile from 40 to 70 degrees. The forward hemisphere of this particle is thus decidedly non-spherical.

Our final example is that of a 38 micron particle which had attached to its surface at least 2 other particles which

were large enough to be directly seen in the near field forward image. This particle also had a bimodal behavior. There was a mode of behavior in which the particle rotated at about 2 - 3 Hz and translated up and down 10 particle diameters along the beam axis. But periodically this wild mode would stop and the particle would hold a stable position for an extended period of time. The results listed in Figure 13 for this particle record only data taken while the particle was in its stable mode. Despite the presense of surface contaminents of significant size, the overall shape of the empirical angular distribution is consistent with that of a sphere of the equivalent size. The biggest departure between empirical and spherical angular distributions seems to be in the relative widths of the maxima around 90 degrees.

PART FOUR: SUMMARY AND DISCUSSION

In these experiments we have, for the first time, made scattering measurements on highly transparent particles in which the radiation which is scattered is also used to support and confine the particle. The trials in which we utilize spherical particles show that our experiment reproduces all the predictions of the Mie theory for scattering by spheres - at least within the limitation of a 2 degree average imposed by the field of view of the goniometer. We note that the large size parameter of the

particles we employ guarantees high sensitivity to the index of refraction and the size of the spheres. We are satisfied that our experimental technique, properly extended, is an excellent way to systematically investigate scattering over a range of size parameters from x = 50 to as much as x = 1000.

The objective of much of our work has been to determine how the scattering from irregular particles differs from that of spheres of the same size. To this end we have mostly employed particles basically spherical in shape in which small particles, both regular and irregular in shape, are attached to the surface. These small particles typically do not exceed 10% of the size of the large particle to which they are attached.

Our first conclusion is that the most significant way in which the irregular particle differs from the equivalent sphere is in the enhancement of radiation scattered into the backward hemisphere relative to that emerging into the forward hemisphere. Detailed structure in the neighborhood of 90 degrees and the nature of the rise beyond 150 degrees also show differences between sphere and irregular particle but those differences could be mimicked by altering the size, index of refraction, or polarization. However the change in ratio of intensities of the two hemispheres seems to be a change that genuinely reflects departure from spherical shape.

A second conclusion is that surface structure results in longitudinal variations in the intensity at fixed scattering angle that can change by a factor of 10 or more as the particle rotates. This is certainly a way in which the spherical and irregular particle differ from one another. We find however that the intensity distribution, uniformly averaged over longitudes of a rotating particle, frequently gives results which look spherical.

Observed motion of particles levitated in ambient atmosphere includes rotation about the beam axis, oscillation about the beam axis, and periodic translation along the beam axis. But the amplitude or frequency of these motions is not found to be correlated to the angular distribution that we have measured. Irregular particles can be locked into a fixed orientation, exhibiting little or no motion and differ strongly from spherical scattering. Rotating particles can give results similar to those of spheres. Our final conclusion then is that the dynamical behavior of the irregular particle in the beam is not a good predictor of how much the angular distribution of the scattered radiation will differ from that of a sphere.

The results we have obtained point the way to many extensions of the current work. The feasibility of a systematic study of scattering using our technique has been established. Among the directions in which this work should be extended are the following:

1. Future redesign of the experiment should extend the range of angles over which we can observe the intensity. We must be able to follow beyond the rise in the backward hemisphere to 170 degrees to search for any potential signature of irregular particles in a region that could not be reached with our current design. Extension to forward angles of say 10 degrees is also highly desirable since we saw some intriguing indications that intensity distributions that are flat in the region 30 to 60 degrees are accompanied by very large and narrow maxima below 30 degrees.

2. The experiment needs to be provided with a more reliable way to capture the particle which is levitated (our success rate was about 30%). In this way we hope to correlate surface structure to both dynamical behavior in levitation and to the angular distribution of scattering. Characterization of irregularities by far field intensity patterns is unreliable compared to the opportunity to examine the actual particle under magnification.

3. We need to redesign our goniometer system into an array of detectors and light baffles each covering a small angular range. In this way rotation of the array by only 10 or 20 degrees will allow us to measure the entire set of interesting scattering angles. The purpose is to permit us to measure an angular

distribution in a much shorter length of time. This is desirable because it is our experience that levitated particles frequently shift their pattern of motion between 2 or 3 modes. This almost always happens too rapidly to complete an angular distribution before the mode changes. The redesign of the goniometer system to make measurements over a shorter interval of time should permit us to make independent measurements of the angular distribution of a given particle in each of its dynamical modes. The significance of this would be to learn how the angular distribution changes when the shape of the particle remains fixed but the orientation of the particle changes with respect to the incident beam.

4. We wish to extend the range of particle shapes under investigation to include cases in which the three dimensions of a particle differ significantly from each other. This will require some investigation into the dynamics of particles in optical traps.

It is the nature of scientific investigation to end the phase of a study with even more questions than were present at the beginning of the study. A new and powerful approach has been opened for the investigation of electromagnetic scattering from particles.

FIGURE CAPTIONS

Figure 1. Optical forces resulting from variations in the intensity profile of the incident radiation for highly transparent and highly reflective particles.

Figure 2. Diagram of the scattering chamber.

Figure 3. 90 degree near field image. From: Ashkin, A. (1972) Scientific American, February, p. 69.

Figure 4. Theoretical scattering from a 39.6 micron transparent sphere based on Mie theory. The high frequency oscillations in this scattering curve are derived from the Mie solution. The dark line running through the center of these oscillations is the expected output of a detector with a 2 degree field of view.

Figure 5. Scattering of (λ=514.5 nm) laser light off of a 33 μm sphere of fused silica. The experimental measurements (dots) are compared to Mie theory (curve).

Figures 6a and 6b. The effect of the direction of polarization of the incident light. Here, the angle of the electric field vector with respect to the normal to the scattering plane is 0 degrees in 6a and 90 degrees in 6b. Experimental results are superimposed for comparison.

Figures 7a-7c. To demonstrate the sensitivity of scattering results to the index of refraction of the particle, experimental measurements are superimposed on theoretical curves differing in index of refraction by .001. This sensitivity allowed us to determine the index of refraction of the glass in our sample o be 1.519.

Figure 8. Experimental scattering measurements for a 25 μm particle compared to Theoretical and values for an equivalent sized sphere sphere.

Figure 9. Experimental scattering measurements for a 51 μm particle compared to Theoretical and values for an equivalent sized sphere sphere.

Figure 10. Experimental scattering measurements for a 35 μm particle compared to Theoretical and values for an equivalent sized sphere sphere.

Figure 11. Experimental scattering measurements for a 45 μm particle compared to Theoretical and values for an equivalent sized sphere sphere.

Figure 12. Experimental scattering measurements for a 55 μm particle compared to Theoretical and values for an equivalent sized sphere sphere.

Figure 13. Experimental scattering measurements for a 38 μm particle compared to Theoretical and values for an equivalent sized sphere sphere.

Figure-1.

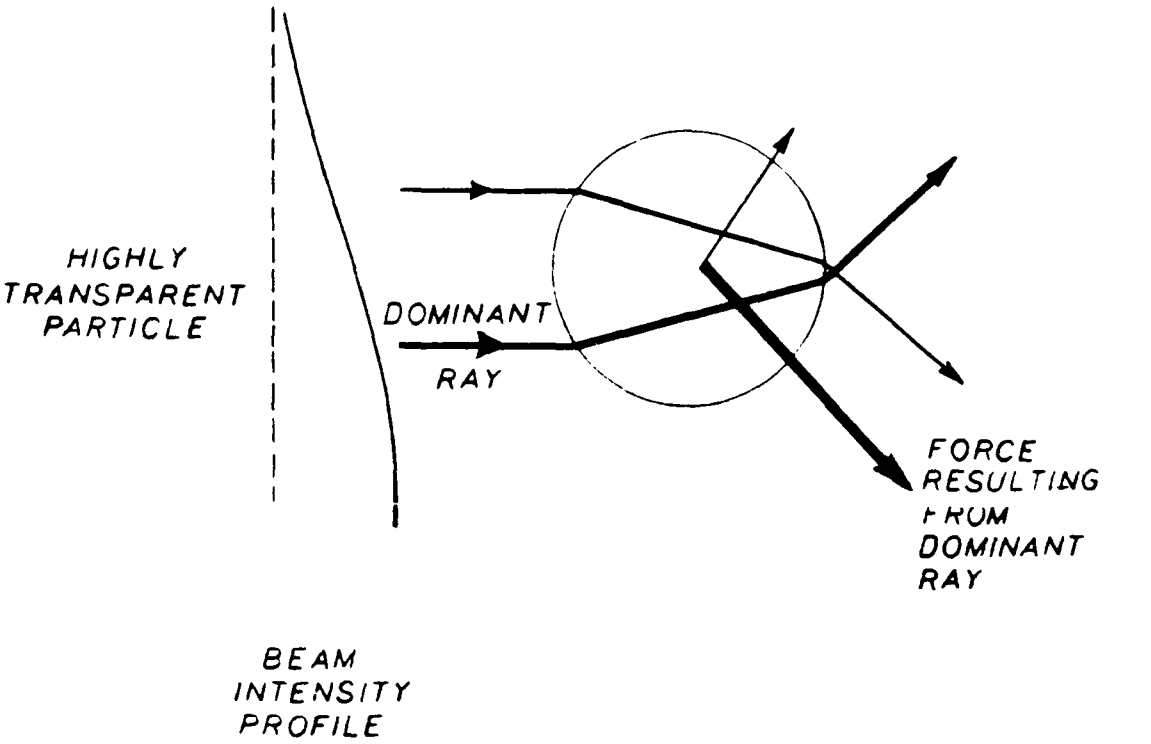
HIGHLY
TRANSPARENT
PARTICLE
DOMINANT
RAY
FORCE
RESULTING
FROM
DOMINANT
RAY
BEAM
INTENSITY
PROFILE

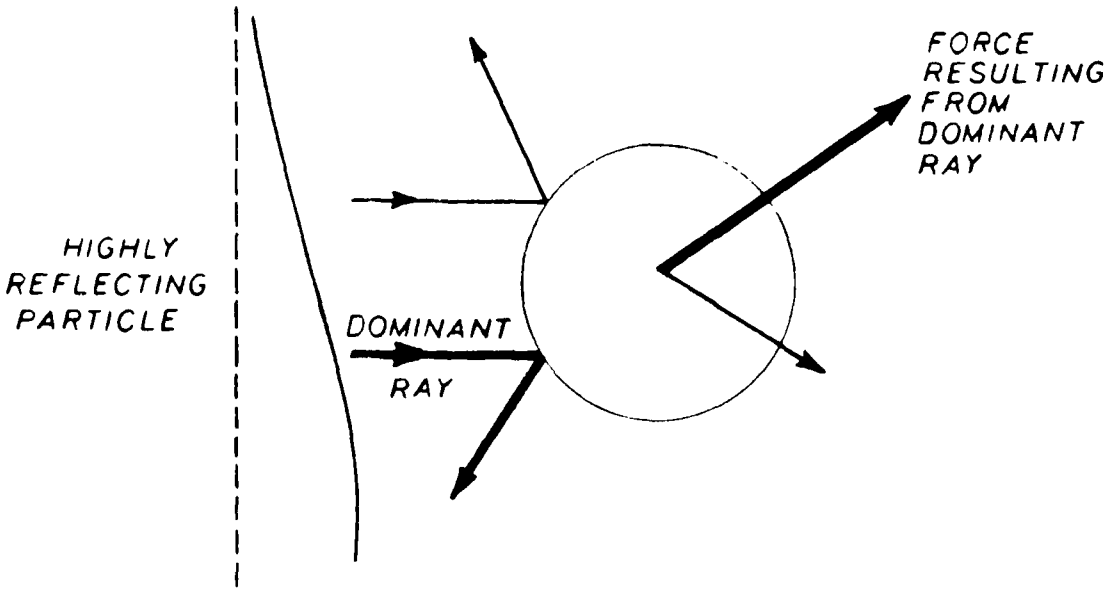
FORCE
RESULTING
FROM
DOMINANT
RAY
HIGHLY
REFLECTING
PARTICLE
DOMINANT
RAY

Figure 2.

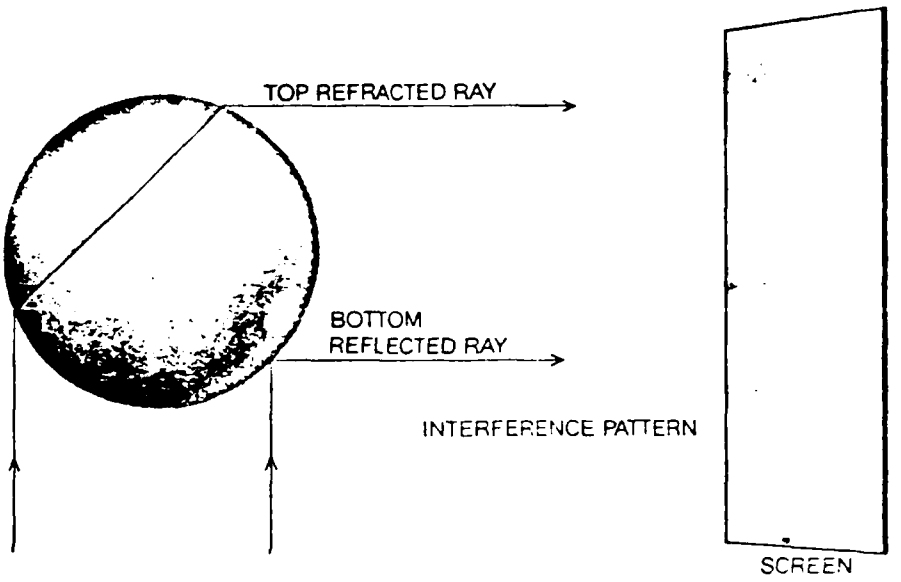
TOP REFRACTED RAY
BOTTOM
REFLECTED RAY
INTERFERENCE PATTERN
SCREEN

Figure 3.

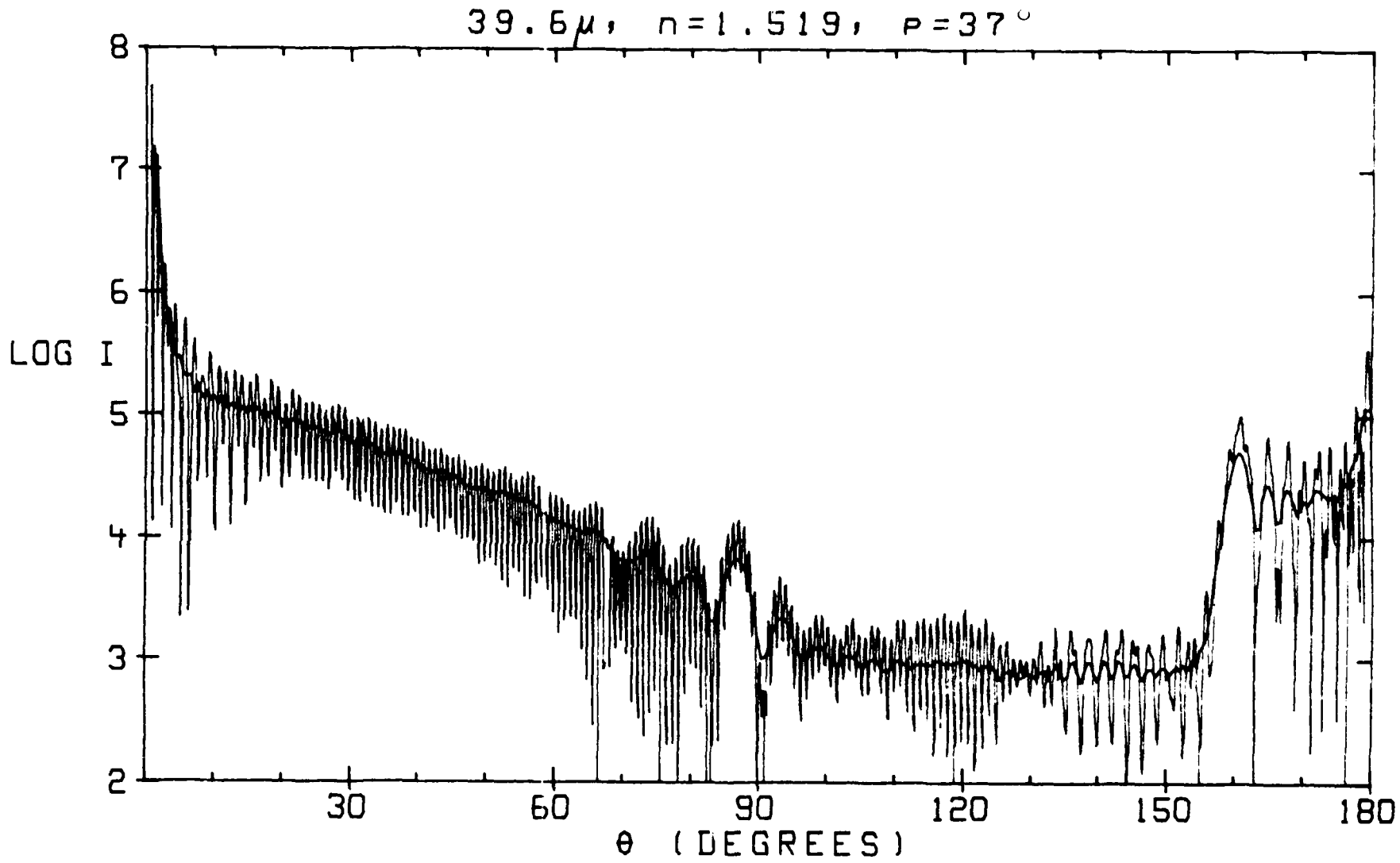

Figure 4.

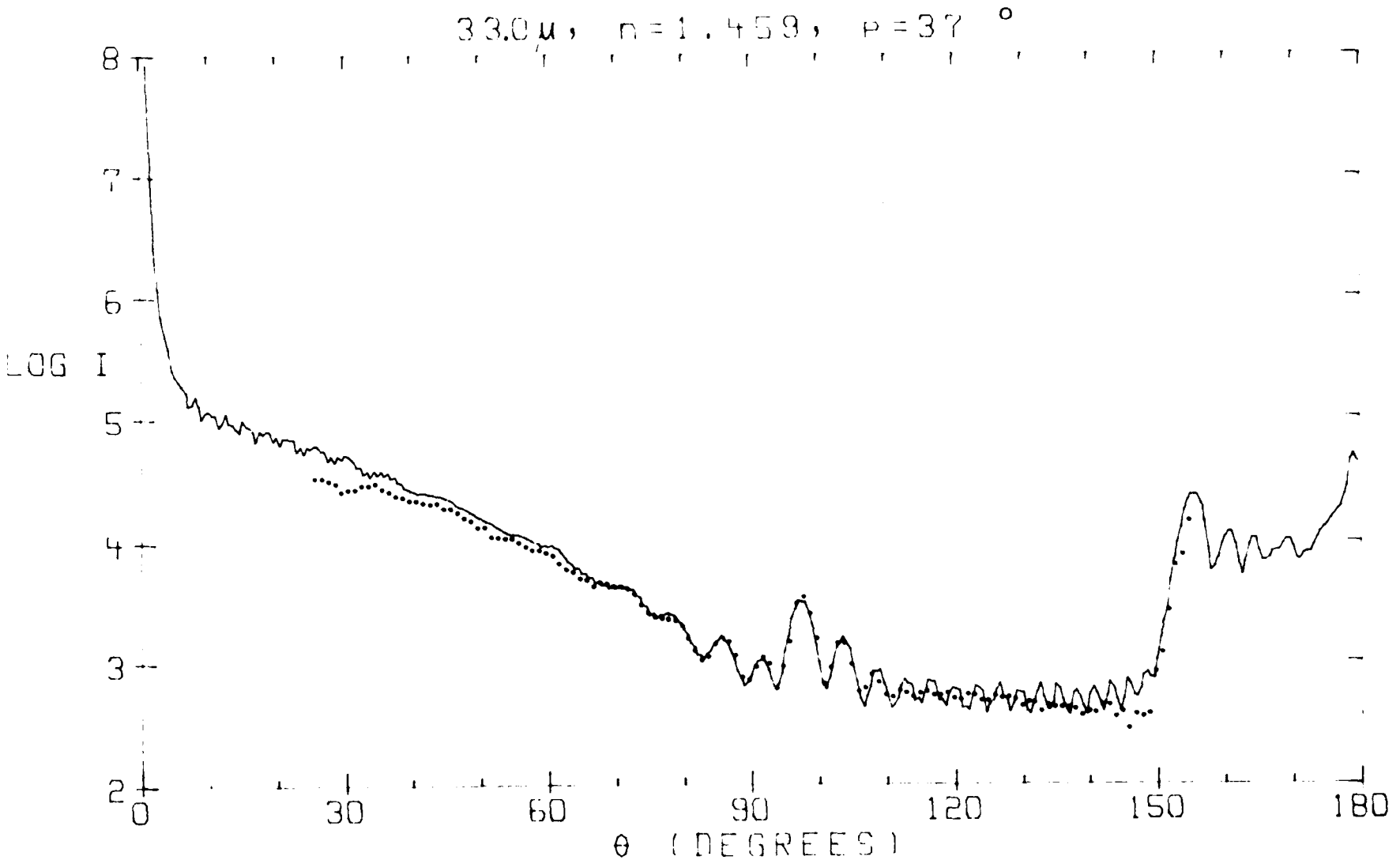

Figure 5.

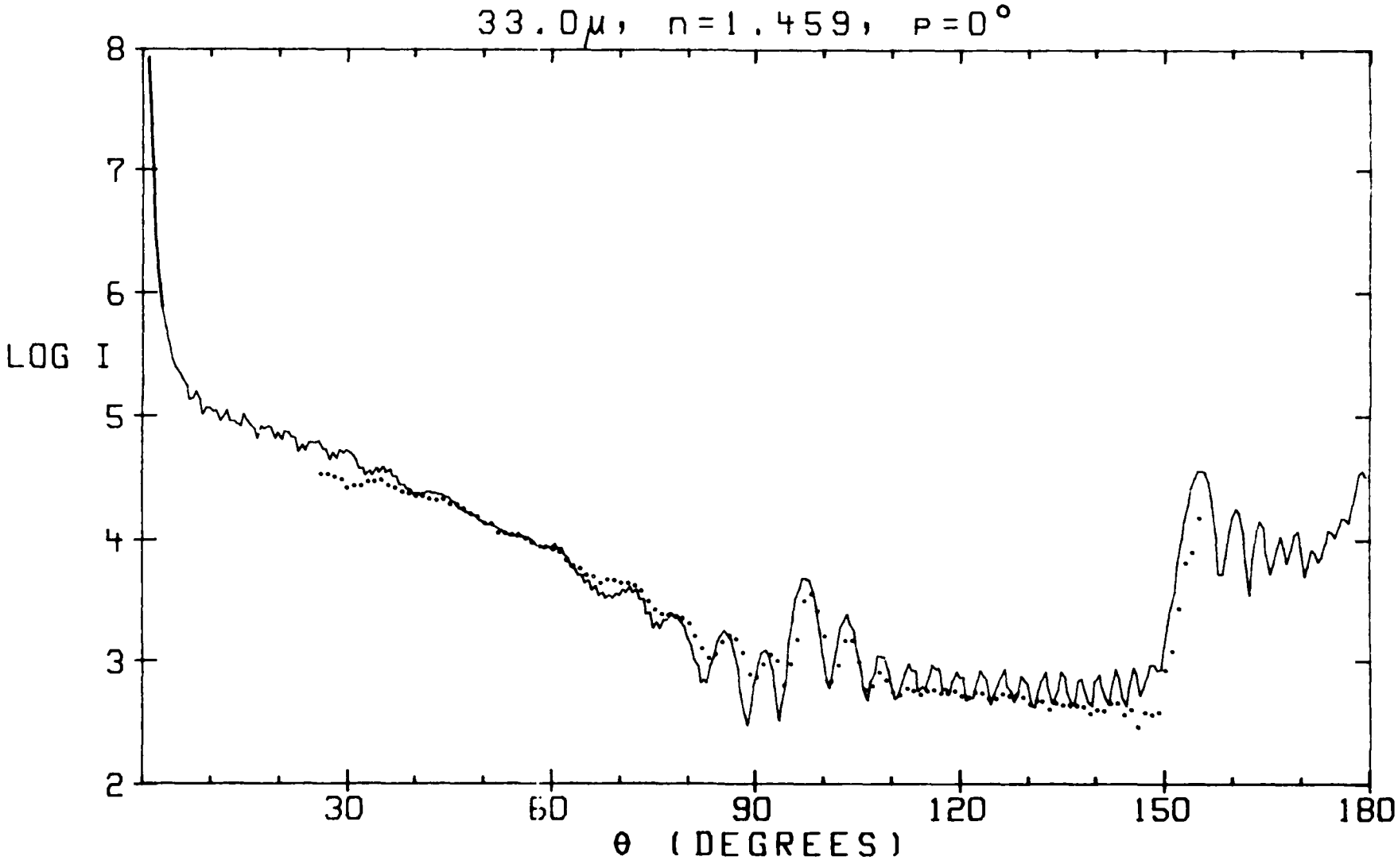

Figure 6a.

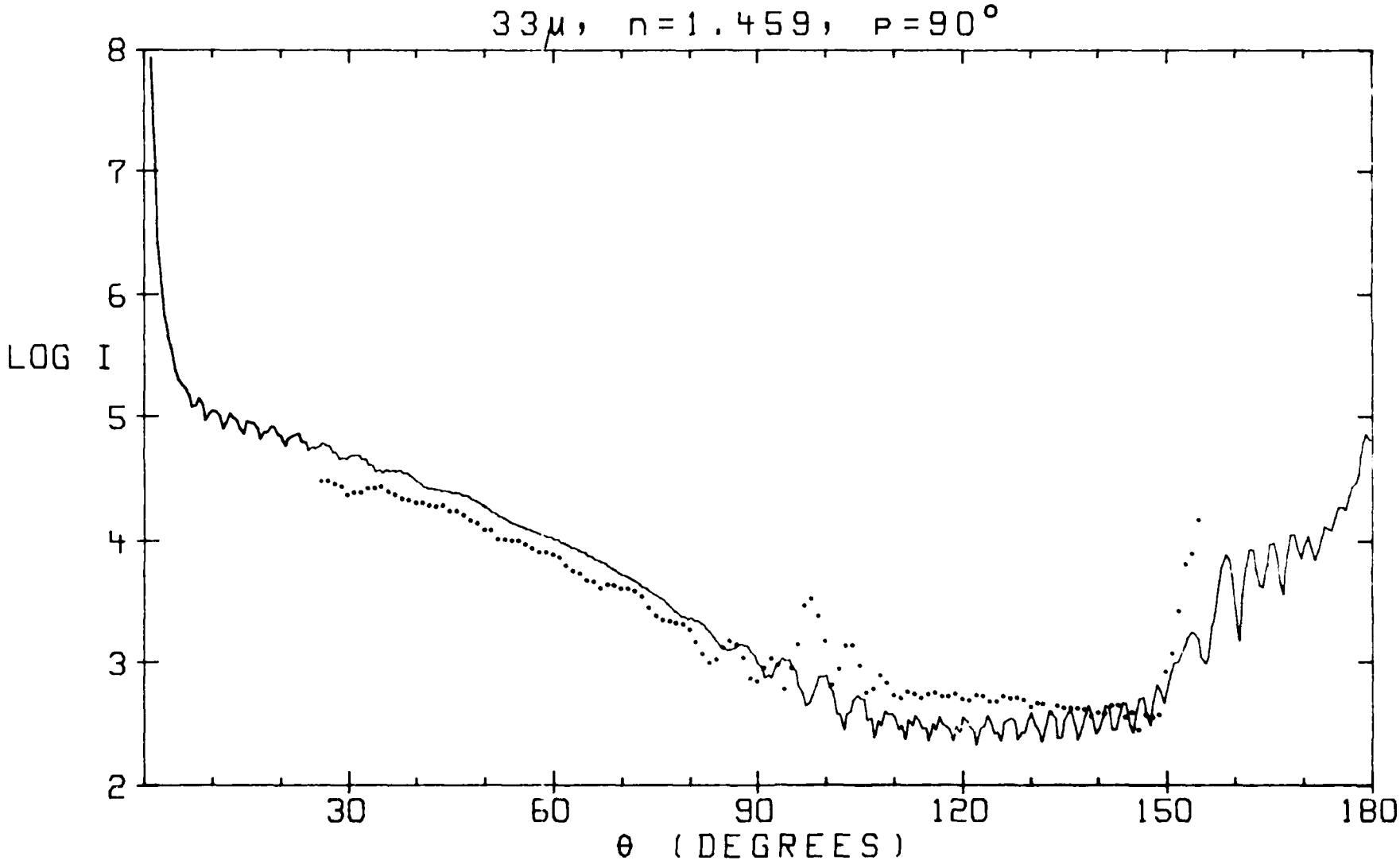

Figure 6b.

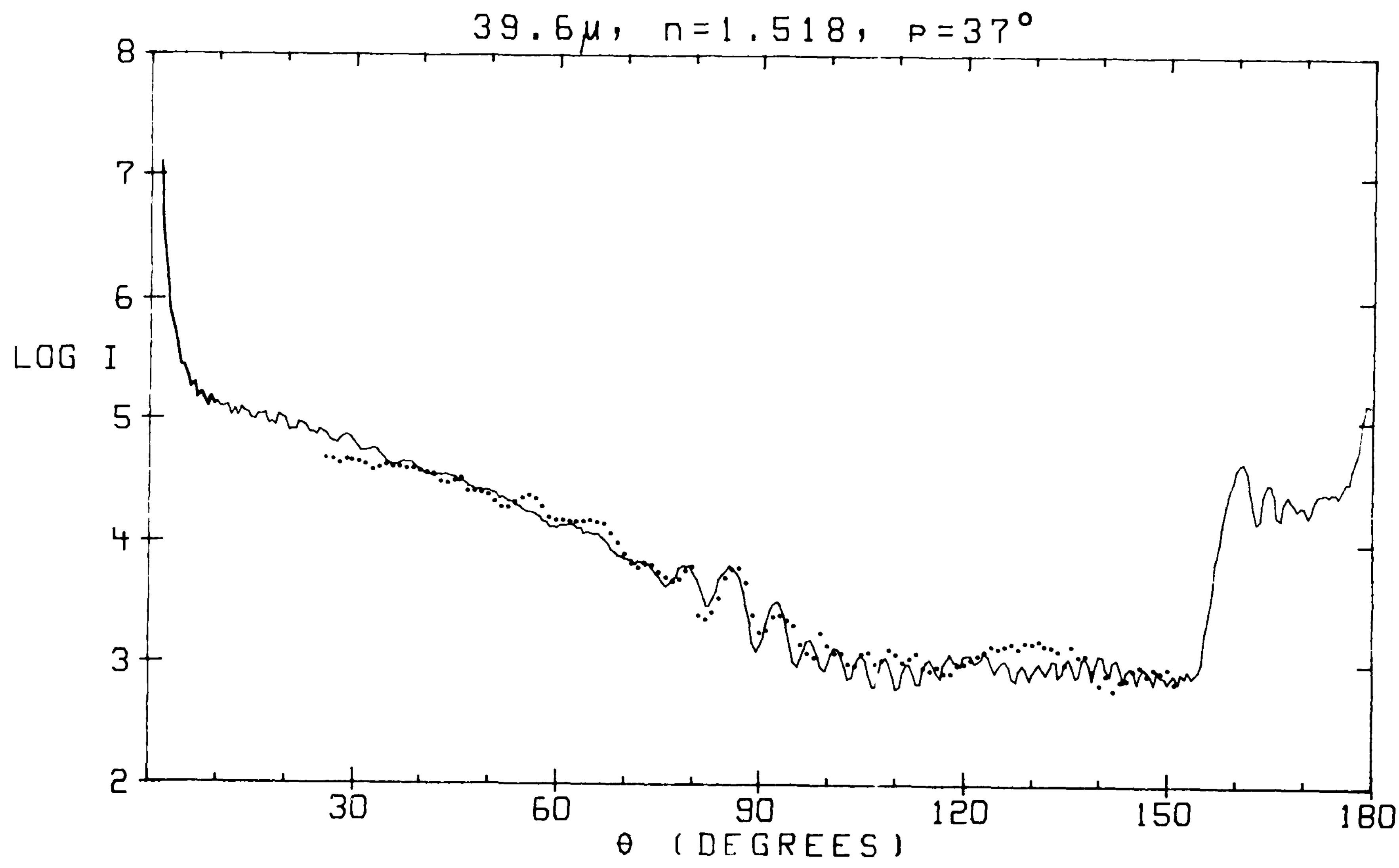

Figure 7a.

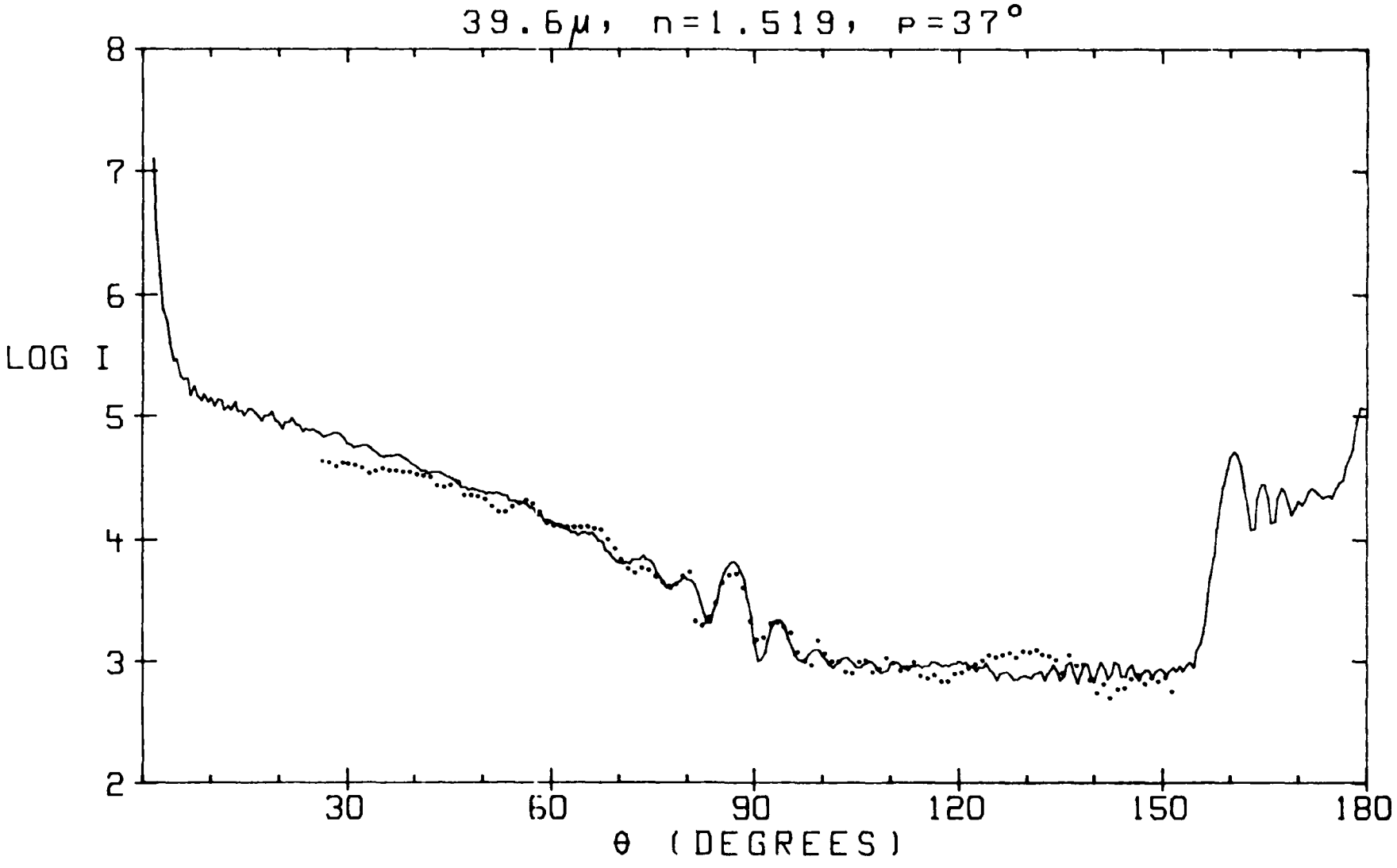

Figure 7b.

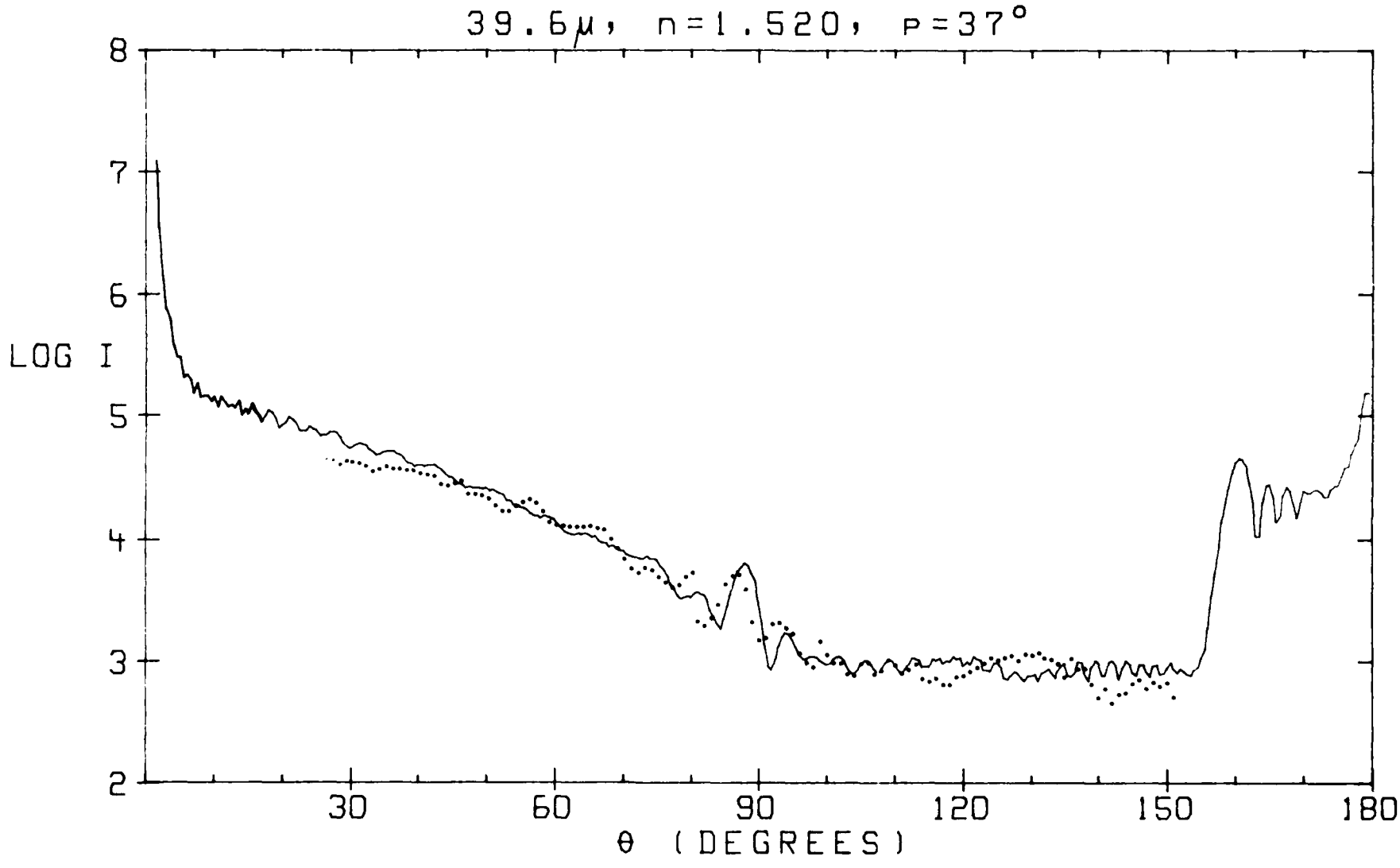

Figure 7c.

Figure 8.

Figure 9.

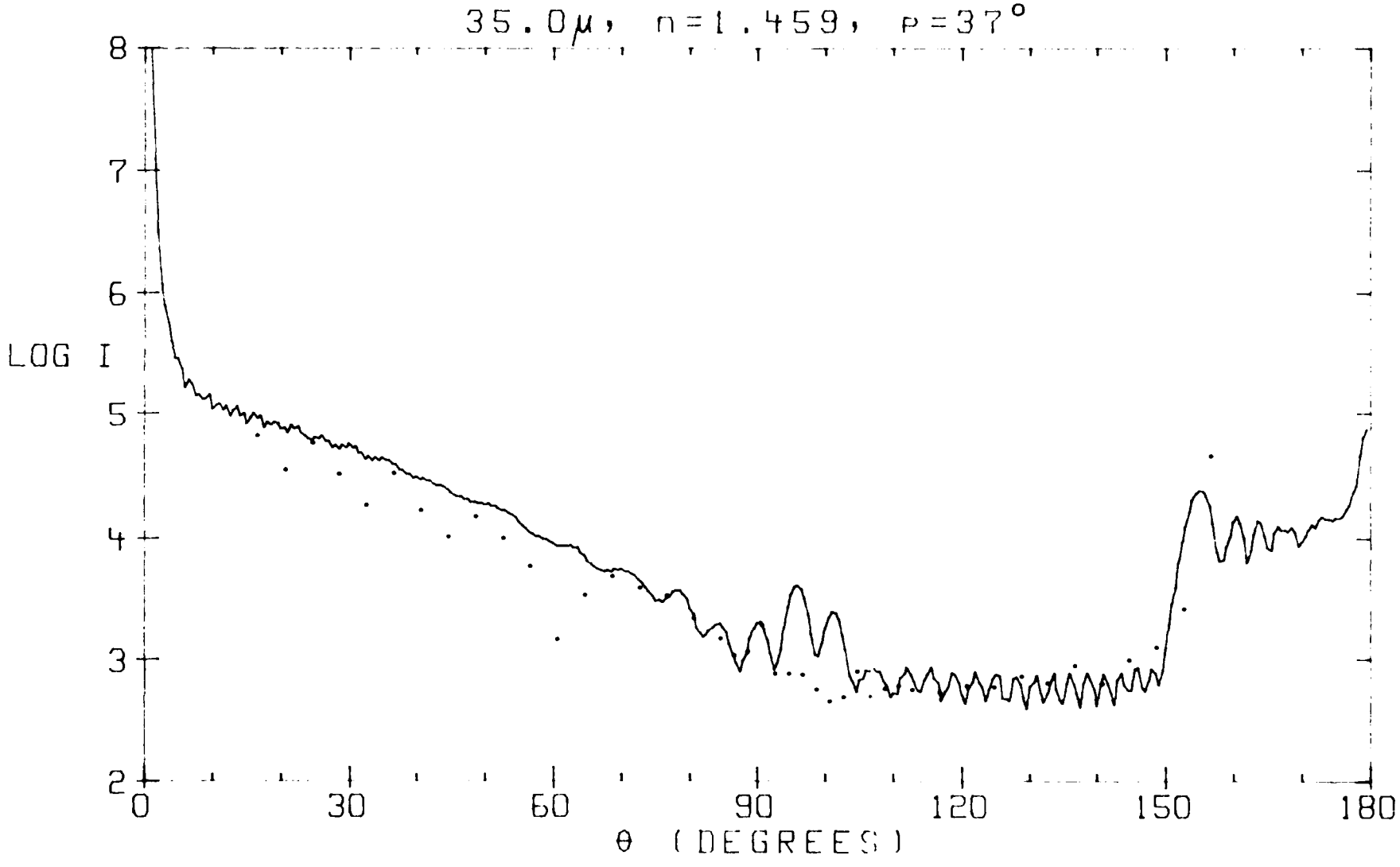

Figure 10.

Figure 11.

LOG I
8
7
6
5
4
3
2
0
30
60
90
120
150
180
θ (DEGREES)
55.0M, n=1.519, P=37°

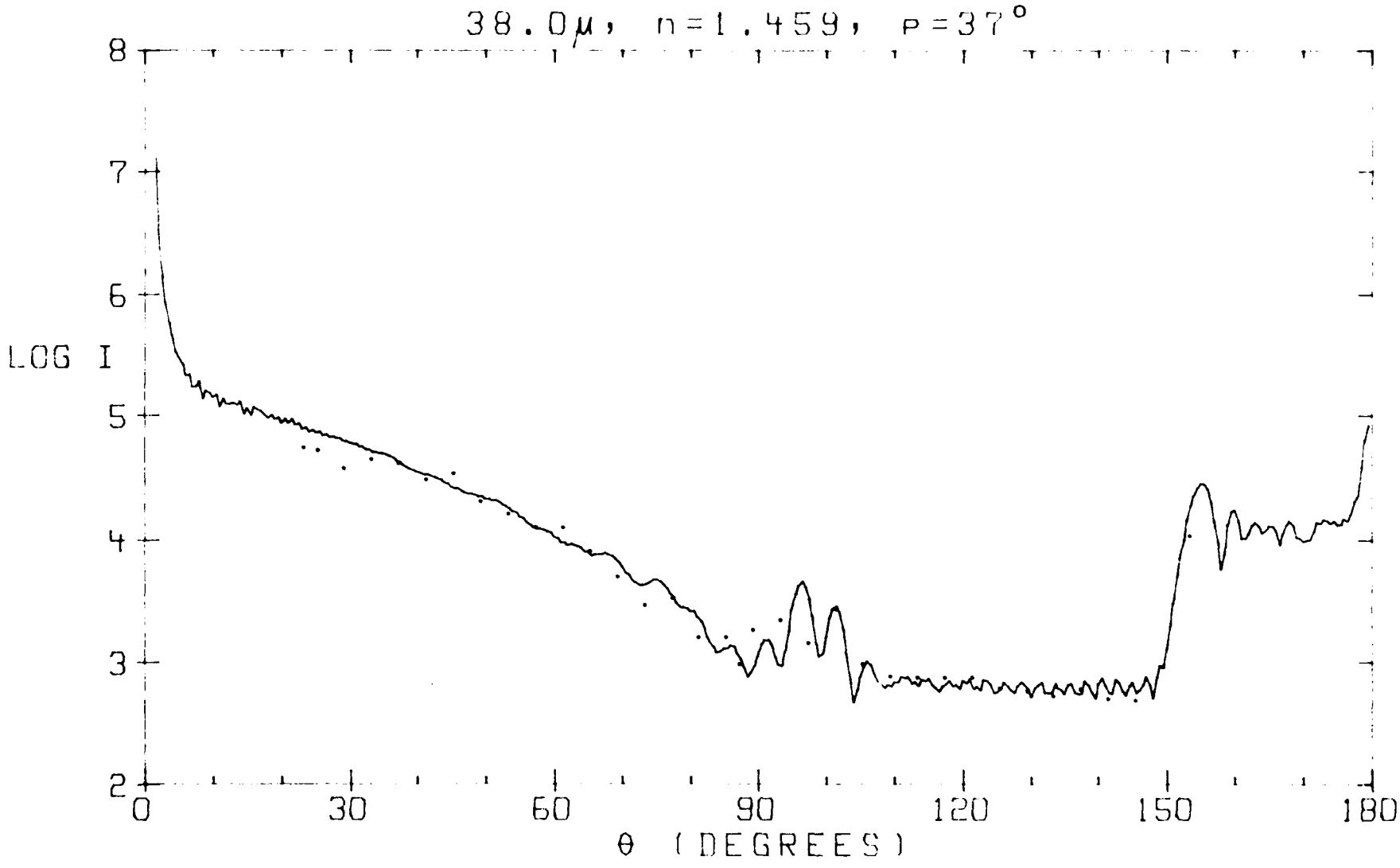

Figure 13.

END

DATE

FILMED

4-88

DTIC